Retardation of arsenic transport through a Pleistocene aquifer

Alexander van Geen[1*], Benjamín C. Bostick[1], Pham Thi Kim Trang[2], Vi Mai Lan[2], Nguyen-Ngoc Mai[2], Phu Dao Manh[2], Pham Hung Viet[2], Kathleen Radloff[1, a], Zahid Aziz[1, b], Jacob L. Mey[1], Mason O. Stahl[3], Charles F. Harvey[3], Peter Oates[4], Beth Weinman[5, c], Caroline Stengel[6], Felix Frei[6], Rolf Kipfer[6], Michael Berg[6]

[1]Lamont-Doherty Earth Observatory of Columbia University, Palisades, NY 10964, USA
[2]CETASD, Hanoi University of Science, Vietnam National University, Hanoi, Vietnam
[3]Massachusetts Institute of Technology, Cambridge, MA 02139, USA
[4]Anchor QEA,Montvale, NJ 07645, USA
[5]Earth & Environmental Sciences, Vanderbilt University, Nashville, TN 37235, USA
[6]Eawag, Swiss Federal Institute of Aquatic Science and Technology, Dübendorf, Switzerland
Final version for *Nature* June 7, 2013

*Corresponding author
E-mail: avangeen@ldeo.columbia.edu
Phone: (845) 365 8644; Fax: (845) 365 8155

Now at:
[a]Gradient, Cambridge, MA 02138, USA
[b]Sadat Associates, Trenton, NJ 08610, USA
[c]Earth and Environmental Sciences, California State University, Fresno, CA 93740, USA

Groundwater drawn daily from shallow alluvial sands by millions of wells over large areas of South and Southeast Asia exposes an estimated population of over 100 million to toxic levels of arsenic (*1*). Holocene aquifers are the source of widespread arsenic poisoning across the region (*2, 3*). In contrast, Pleistocene sands deposited in this region more than ~12,000 years ago mostly do not host groundwater with high levels of arsenic. Pleistocene aquifers are increasingly used as a safe source of drinking water (*4*) and it is therefore important to understand under what conditions low levels of arsenic can be maintained. Here we reconstruct the initial phase of contamination of a Pleistocene aquifer near Hanoi, Vietnam. We demonstrate that changes in groundwater flow conditions and the redox state of the aquifer sands induced by groundwater pumping caused the lateral intrusion of arsenic contamination over 120 m from Holocene aquifer into a previously uncontaminated Pleistocene aquifer. We also find that arsenic adsorbs onto the aquifer sands and that there is a 16-20 fold retardation in the extent of the contamination relative to the reconstructed lateral movement of groundwater over the same period. Our findings suggest that arsenic contamination of Pleistocene aquifers in South and Southeast Asia as a consequence of increasing levels of groundwater pumping have been delayed by the retardation of arsenic transport.

This study reconstructs the initial phase of contamination of a low-As aquifer in a village 10 km southeast of Hanoi on the banks of the Red River. A key feature of the site is the juxtaposition of a high-As aquifer upstream of a low-As aquifer in an area where pumping for the city of Hanoi has dominated lateral groundwater flow for the past several decades (Fig. 1A). Many residents of the village of Van Phuc where the site is located still draw water from their 30 to 50 m-deep private wells. In the western portion of the village, the wells typically contain <10 µg/L As and therefore meet the World Health Organization (WHO) guideline for in drinking water, whereas As in groundwater from most wells in eastern Van Phuc exceeds this guideline by a factor of 10-50 (*5*). Drilling and sediment dating in the area has shown that low-As groundwater is drawn from orange-colored sands deposited over 12,000 years ago, whereas high-As groundwater is typically in contact with grey sands deposited less than 5,000 years ago (*6-7*). The key issue addressed in this study is to what extent the boundary between the low- and high-As aquifers of Van Phuc has shifted in response to groundwater withdrawals in Hanoi. This unintended full-scale experiment spanning several decades has implications for low-As aquifers throughout Asia that are vulnerable to contamination due to accelerated groundwater flow.

The collection of sediment cores and installation of monitoring wells was concentrated along a southeast to northwest-trending transect that extends over a distance of 2.2 km from the bank of the Red River (Fig. 1B). Groundwater heads, and therefore the groundwater velocity field, within Van Phuc rapidly respond to the daily and seasonal cycles of the river stage (Supplementary Information). Before large-scale groundwater withdrawals, rainfall was sufficient to maintain groundwater discharge to the river, as is still observed elsewhere along the Red River (*8*). In Van Phuc, however, the groundwater level was on average 40 cm below that of the Red River stage in 2010-11 and the hydraulic gradient nearly always indicated flow from the river into the aquifer. The reversal of the natural head gradient is caused by the large depression in groundwater level centered 10 km to the northwest that induces groundwater flow along the Van Phuc transect from the river towards Hanoi (Fig. 1A). This perturbation of groundwater flow is caused by massive pumping for the municipal water supply of Hanoi (*9-11*), which nearly doubled from 0.55 to 0.90 x 10^6 m^3/day between 2000 and 2010 due to the rapid expansion of the city (Fig. S1).

A change in the color of a clay layer capping sandy sediment along the transect defines a geological boundary between the two portions of the Van Phuc aquifer. Up to a distance of 1.7 km from the river bank, the clay capping the aquifer is uniformly grey with the exception of a thin brown interval at the very surface (Fig. 2B). In contrast, a readily identifiable sequence of highly oxidized bright yellow, red, and white clays was encountered between 12 and 17 m depth at all drill sites along the transect beyond a distance of 1.7 km from the river bank. This oxidized clay layer is probably a paleosol dating to the last sea level low-stand ~20,000 years ago (*7*, *12*).

The color of aquifer sands below the upper clay layer also changes markedly along the Van Phuc transect. Sand color in fluvio-deltaic deposits is controlled primarily by the extent to which Fe(III) has been reduced to Fe(II) by the decomposition of organic carbon (*13*). Up to a distance of 1.6 km from the river bank, sandy drill cuttings within the 20-40 m depth range are uniformly grey. The predominance of orange sands beyond 1.6 km indicates oxidation during the previous sea level low-stand. After sea level rose back to its current level, the nature of the remaining organic carbon precluded a new cycle of Fe(III) reduction (*14*).

Independently of sediment color, the calcium (Ca) content of sand cuttings collected while drilling along the Van Phuc transect confirms that a geological boundary extends to the underlying aquifer sands. Within the southeastern portion of the aquifer that is not capped by the presumed paleosol, X-ray fluorescence measurements indicate Ca concentrations >2,000 mg/kg in sand cuttings to a depth of 30 m (Fig. 2A). The groundwater in this portion of the aquifer is supersaturated with respect to calcite and dolomite (*6*), suggesting that authigenic precipitation is the source of Ca in the grey drill cuttings, as previously proposed elsewhere (*12*) (Fig. S2). At a distance of 1.7 km from the river and further to the northwest, instead, the Ca content of orange sand cuttings systematically remains <100 mg/kg and the groundwater is undersaturated with respect to calcite and dolomite. Unlike surficial shallow grey clays, the Ca content of the presumed paleosol is also very low (<100 mg/kg) and consistent with extensive weathering.

The redox state of the aquifer has a major impact on the composition of groundwater in Van Phuc, as reported elsewhere in Vietnam (*15*) and across South and East Asia more generally (*3*). High Fe (II) concentrations in groundwater (10-20 mg/L) associated with grey reducing sediments are apparent to residents of eastern Van Phuc as an orange Fe(III) precipitate that forms in their water upon exposure to air (Fig. S3). Invisible, but instead constituting a major health threat, are groundwater As concentrations at 20-30 m depth within the same portion of the transect that range from 200 µg/L near the river to levels as high 600 µg/L between 1.2 and 1.6 km from the river bank (Fig. 2C). The groundwater in contact with Pleistocene sands in northwestern Van Phuc is also anaerobic but contains <0.5 mg/L Fe (II) and <10 µg/L As and shows little indication of organic carbon mineralization compared to the Holocene aquifer (Fig. S4).

The Pleistocene portion of the Van Phuc aquifer adjacent to the Holocene sediment is not uniformly orange or low in As. Of particular interest is a layer of grey sand between 25-30 m depth extending to the northwest at a distance of 1.7 to 1.8 km from the river bank (Fig. 2B). The intercalation of grey sand between orange sands above and below, combined with the low Ca content of sand cuttings within this layer, indicate that it was deposited during the Pleistocene and therefore until recently oxidized and orange in color. Within the portion of the Pleistocene aquifer that turned grey and is closest to the geological boundary, groundwater As concentrations are therefore presumed to have been originally very low (<5 µg/L). Actual As concentrations of 100-500 µg/L, as high as in the adjacent Holocene aquifer, indicate contamination extending over a distance of ~120 m into the Pleistocene aquifer (Fig. 3A).

A subset of the transect wells was sampled in 2006 and analyzed for tritium (^{3}H) as well as noble gases in order to measure groundwater ages and determine the rate of As intrusion into the Pleistocene aquifer. Atmospheric nuclear weapons testing in the 1950s and 1960s is the main source of ^{3}H that entered the hydrological cycle (*16*). The distribution of ^{3}H indicates that only groundwater in the southeastern high-As portion of the aquifer contains a plume of recharge dating from the 1950s and later. Concentrations of ^{3}He, the stable decay-product of ^{3}H, were used to calculate groundwater ages for 8 wells in the 24-42 m depth range with detectable levels of ^{3}H. In 2006, the oldest water dated by the ^{3}H-^{3}He method (Fig. S5) was sampled at a distance of 1.6 km from the river, which is the northwestern-most location along the transect where the aquifer is uniformly grey (Figs. 2B, D). Younger ages of 15 and 17 years were measured closer to the river at 1.3 and 1.5 km, respectively. Concentrations of ^{3}H, groundwater ^{3}H-^{3}He ages, and

hydraulic head gradients consistently indicate that the Holocene aquifer has been recharged by the river from the southeast within the last few decades.

Drilling and geophysical data indicate that the main groundwater recharge area extends from the center of the Red River to the inland area where a surficial clay layer thickens markedly, i.e. from 100 m southeast to 300 m northwest of the river bank (Fig. S6). The relationship between groundwater ages and travel distance from the recharge area implies accelerating flow drawn by increased Hanoi pumping (Fig. S7). A simple transient flow model for the Van Phuc aquifer yields average advection rates of 38 and 48 m/yr towards Hanoi since 1951 and 1971, respectively (Supplementary Discussion). According to these two pumping scenarios, groundwater originating from the Holocene portion of the aquifer was transported 2,000-2,300 m into the Pleistocene sands by 2011, when the transect was sampled for analysis of As and other groundwater constituents.

The sharp decline in As concentrations between distances of 1.60 and 1.75 km from the river bank indicates that migration of the As front across the geological boundary was retarded by a factor of 16 to 20 relative to the movement of the groundwater (Fig. 3A). Without retardation, attributable to As adsorption onto aquifer sands, the entire Pleistocene aquifer of Van Phuc would already be contaminated. The retardation is derived from several decades of perturbation and is at the low end of previous estimates by other methods, typically measured within days to weeks (*17-22*), and therefore predicts greater As mobility than most previous studies. The retardation measured in Van Phuc integrates the effect of competing ions typically present at higher concentrations in the Holocene aquifer (Fig. S4) as well as the impact of Fe oxyhyroxide reduction. However, the extent to which contamination was caused by As transport from the adjacent Holocene aquifer or reductive dissolution of Fe(III) oxyhydroxides and *in situ* As release to groundwater cannot be determined from the available data (Fig. S8).

The sharp drop in DOC concentrations across the geological boundary from 9 to ~1 mg/L indicates rapid organic carbon mineralization coupled to the reduction of Fe(III) oxyhydroxides and explains the formation of a plume of grey sands within the Pleistocene aquifer (Fig. 3B). On the basis of a stoichiometric Fe/C ratio of 4 (*15*), the DOC from about 30 pore volumes of flushing with groundwater from the Holocene aquifer would be required to turn Pleistocene sands from orange to grey by reducing half of their 0.1% reactive Fe(III) oxyhydroxide content (*23*), assuming a porosity of 0.25. Given that groundwater was advected over a distance of 2,000-2,300 m across the geological boundary over the past 40-60 years, the plume of grey sands would be predicted to extend 65-75 m into the Pleistocene aquifer. This is somewhat less than observed (Fig. 3), possibly due to additional reduction by H_2 advected from the Holocene portion of the aquifer (*14*). The Van Phuc observations indicate that DOC advected from a Holocene aquifer can be at least as important for the release of As to groundwater as autochthonous organic carbon (*12, 24-27*).

Contamination of Pleistocene aquifers has previously been invoked in the Red River and the Bengal basins (*11-12, 28*), but without the benefit of a well-defined hydrogeological context. The Pleistocene aquifer of Van Phuc was contaminated under the conducive circumstances of accelerated lateral flow. Although downward groundwater flow and therefore penetration of As will typically be slower, the Van Phuc findings confirm that the vulnerability of Pleistocene

aquifers will depend on the local spatial density of incised paleo-channels that were subsequently filled with Holocene sediments (*12*). Due to retardation, concentrations of As in a Pleistocene aquifer will not increase suddenly but over time scales of decades even in close vicinity of a Holocene aquifer. This is consistent with the gradual increase in groundwater As concentrations documented by the few extended time series available from such a vulnerable setting (*29*). However, concentrations of As could rise more rapidly if flow accelerates beyond the rate documented in Van Phuc, closer to Hanoi for instance.

Methods summary

A total of 41 wells were installed in Van Phuc in 2006-11. Water level data of the river and in the wells were recorded from September 2010 to June 2011 using pressure transducers and adjusted to the same elevation datum after barometric corrections. The magnitude and direction of the head gradient within the 25-30m depth interval was calculated from water level measurements in three wells (Fig. 1B). In 2006, a subset of the wells was sampled for noble gas and tritium (^{3}H) analysis at a high flow rate using a submersible pump to avoid degassing. The samples were analyzed by mass spectrometry in the Noble Gas Laboratory at ETH Zurich. ^{3}H concentrations were determined by the ^{3}He ingrowth method (*30*). Groundwater As, Fe, and Mn concentrations measured by high-resolution inductively-coupled plasma mass spectrometry at LDEO represent the average for acidified samples collected in April and May 2012. Further details are provided in the Supplementary Information.

References

1. Ravenscroft, P., Brammer, H. & K. Richards, *Arsenic Pollution: A Global Synthesis* (RGS-IBG Book Series,Wiley-Blackwell, Chichester, UK, 2009)
2. BGS/DPHE (British Geological Survey, Dept. of Public Health Engineering). *Arsenic Contamination of Groundwater in Bangladesh*, Final Report (British Geological Survey, 2001).
3. Fendorf, S., Michael, H. A. & van Geen, A. Spatial and temporal variations of groundwater arsenic in south and southeast Asia. *Science* **328**, 1123-1127 (2010).
4. Ahmed, M. F. *et al.* Epidemiology: Ensuring safe drinking water in Bangladesh. *Science* **314**, 1687-1688 (2006).
5. Berg, M. *et al.,* Magnitude of arsenic pollution in the Mekong and Red River deltas - Cambodia and Vietnam. *Science of the Total Environment* 372, 413 (2007).
6. Eiche, E. *et al.* Geochemical processes underlying a sharp contrast in groundwater arsenic concentrations in a village on the Red River delta, Vietnam. *Applied Geochemistry* **23**, 3143-3154, 2008.
7. Funabiki, A., Haruyama, S., Quy N. V., Hai, P. V., Thai, D. H., Holocene delta plain development in the Song Hong (Red River) delta, Vietnam, *Journal of Asian Earth Sciences* **30**, 518-529 (2007).
8. Larsen, F. *et al.,* Controlling geological and hydrogeological processes in an arsenic contaminated aquifer on the Red River flood plain, Vietnam. *Applied Geochemistry* **23**, 3099-3115 (2008).
9. Thu, T. M. & Fredlund, D. G. Modelling subsidence in the Hanoi City area, Vietnam. *Can. Geotech. J.* **37**, 621-637 (2000).
10. Berg, M. *et al.* Hydrological and sedimentary controls leading to arsenic contamination of groundwater in the Hanoi area, Vietnam: The impact of iron-arsenic ratios, peat, river bank deposits, and excessive groundwater abstraction. *Chemical Geology* **249**, 91-112 (2008).

11. Winkel, L. H. E. *et al.* Arsenic pollution of groundwater in Vietnam exacerbated by deep aquifer exploitation for more than a century. *Proc. Natl Acad. Sci. USA* **108**, 1246-1251 (2011).
12. McArthur, J. M. *et al.* How paleosols influence groundwater flow and arsenic pollution: A model from the Bengal Basin and its worldwide implication. *Water Resour. Res.* **44**, W11411, doi:10.1029/2007WR006552 (2008).
13. Horneman, A., *et al.* Decoupling of As and Fe release to Bangladesh groundwater under reducing conditions. Part I: Evidence from sediment profiles. *Geochim. Cosmochim. Acta* **68**, 3459-3473 (2004).
14. Postma, D. *et al.* Groundwater arsenic concentrations in Vietnam controlled by sediment age. *Nature Geoscience* **5**, 656-661(2012).
15. Postma, D. *et al.* Arsenic in groundwater of the Red River floodplain,Vietnam: Controlling geochemical processes and reactive transport modeling. *Geochim. Cosmochim. Acta* **71**, 5054-5071 (2007).
16. Kipfer, R., Aeschbach-Hertig, W., Peeters, F. & Stute, M. Noble gases in lakes and ground waters. *Rev. Mineral. Geochem.* **47**, 615-700 (2002).
17. Stollenwerk, K. G. *et al.* Arsenic attenuation by oxidized aquifer sediments in Bangladesh. *Sci. Total Environ.* **379**, 133-150 (2007).
18. van Geen, A. *et al.* Flushing history as a hydrogeological control on the regional distribution of arsenic in shallow groundwater of the Bengal Basin. *Environ. Sci. Technol.* **42**, 2283-2288 (2008).
19. Nath, B *et al.* Mobility of arsenic in the sub-surface environment: An integrated hydrogeochemical study and sorption model of the sandy aquifer materials, *Journal of Hydrology* **364**, 236–248 (2009).
20. Itai, T. *et al.* Variations in the redox state of As and Fe measured by X-ray absorption spectroscopy in aquifers of Bangladesh and their effect on As adsorption. *Appl. Geochem.* **25**, 34–47 (2010).
21. Radloff, K. A. *et al.*, Arsenic migration to deep groundwater in Bangladesh influenced by adsorption and water demand. *Nature Geoscience* 4, 793–798 (2011).
22. Jessen, S. *et al.* Surface complexation modeling of groundwater arsenic mobility: Results of a forced gradient experiment in a Red River flood plain aquifer, Vietnam. *Geochim. Cosmochim. Acta* **98**, 186-201 (2012).
23. Dhar, R. K *et al.* Microbes enhance mobility of arsenic in Pleistocene aquifer sand from Bangladesh. *Environ. Sci. Technol.* **45**, 2648-2654 (2011).
24. Islam, F. S. *et al.* Role of metal-reducing bacteria in arsenic release from Bengal delta sediments. *Nature* **430**, 68-71 (2004).
25. Polizzotto, M. L., Kocar, B. D., Benner, S. B., Sampson, M. & Fendorf, S. Near-surface wetland sediments as a source of arsenic release to ground water in Asia. *Nature* **454**, 505-508 (2008).
26. Neumann, R. B. *et al.* Anthropogenic influences on groundwater arsenic concentrations in Bangladesh. *Nature Geosci.* **3**, 46-52 (2010).
27. Mailloux, B. J. *et al.* Advection of surface-derived organic carbon fuels microbial reduction in Bangladesh groundwater. *Proc. Natl. Acad. Sci. USA*, doi: 10.1073/pnas.1213141110 (2013).
28. Mukherjee, A. *et al.* Elevated arsenic in deeper groundwater of the western Bengal basin, India: Extent and controls from regional to local scale. *Appl. Geochem.* **26**, 600-613 (2011).

29. McArthur, J. M. *et al.* Migration of As, and ^{3}H-^{3}He ages, in groundwater from West Bengal: Implications for monitoring. *Wat. Res.* **44**, 4171-4185 (2010).
30. Beyerle, U. *et al.,* A mass spectrometric system for the analysis of noble gases and tritium from water samples, *Environ. Sci. Technol.* 34, 2042-2050 (2000).

Acknowledgements:
This study was supported by NSF grant EAR 09-11557, the Swiss Agency for Development and Cooperation, grant NAFOSTED 105-09-59-09 to CETASD, and NIEHS grants P42 ES010349 and P42 ES01645. This is Lamont-Doherty Earth Observatory contribution number 7698.

Author contributions:
A.v.G, M.B., P.T.K.T., P.O., and B.B. conceived the study. V.M.L., N.N.M, P.D.M., P.T.K.T., and P.H.V. were responsible for organizing the field work and carrying out the monitoring throughout the study. K.R., Z.A, and B.W. participated in the field work in 2006. M.O.S. processed the hydrological data and carried out the flow modeling under the supervision of C.F.H. and P.O. J.L.M. was responsible for groundwater analyses at LDEO, C.S. at Eawag, and F.F. for noble gas measurements in R.K.'s laboratory. A.v.G drafted the paper, which was then edited by all co-authors.

Author information:
Reprints and permissions information is available at www.nature.com/reprints. The authors have no competing financial interests to declare. Correspondence and requests for materials should be addressed to avangeen@ldeo.columbia.edu.

Figure captions:

Figure 1 Map of the Hanoi area extending south to the study site. (A) Location of the village of Van Phuc in relation to the cone of depression formed by groundwater pumping for the municipal water supply of Hanoi (adapted from (*10*)). Urbanized areas are shown in grey; largely open fields are shown in green. (B) Enlarged view of Van Phuc from Google Earth showing the location of the transect along which groundwater and sediment were collected, with tick marks labels indicating distance from the Red River bank in kilometers. Symbol color distinguishes the uniformly grey Holocene aquifer (red), the Pleistocene aquifer contaminated with As (yellow), the Pleistocene aquifer where the groundwater conductivity and DIC concentrations are high but As concentrations are not (green), and the Pleistocene aquifer without indication of contamination (blue), all within the 25-30 m depth interval. Three white asterisks identify the wells that were used to determine flow direction. (C) Rose diagram frequency plot of the head gradient direction based on data collected at 5 min intervals on these three wells from September 2010 through June 2011.

Figure 2 Contoured sections of sediment and water properties based on data collected between distances of 1.3 and 2.0 km from the Red River bank. The location and number of samples indicated as black dots varies by type of measurement. (A) Concentration of Ca in sand cuttings measured by X-ray fluorescence. Also shown are the boundaries separating the two main aquifers and the paleosol overlying the Pleistocene aquifer. (B) Difference in diffuse spectral reflectance between 530 and 520 nm indicative of the color of freshly collected drill cuttings (*13*), (C) concentrations of As in groundwater collected in 2006 with the needle-sampler and in 2011 from monitoring wells along the transect. (D) Groundwater ages relative to recharge determining by ^{3}H-^{3}He dating of groundwater samples collected from a subset of the monitoring wells in 2006. The portion of the Pleistocene aquifer that became reduced and where As concentrations presumably increased over time is located within the large arrow pointing in the direction of flow.

Figure 3 Distribution of (A) arsenic and (B) dissolved organic carbon in groundwater within the 25-30 m depth interval along the Van Phuc transect. Symbols are colored according to the classification in Fig. 1. Grey and yellow shading indicates the extent of the grey Holocene aquifer and the portion of the Pleistocene aquifer that is still orange, respectively. The intermediate area without shading indicates the portion of the Pleistocene aquifer that turned grey. Shown as dotted lines are predicted As concentrations bracketing the observations with retardation factors of 16 and 20 and an average advection velocity of 43 m/yr over the 50 years preceding the 2011 sampling (Supplementary Discussion). Also shown are predicted concentrations for As assuming retardation factors of 5 and 50 and the same average rate of advection. For visual reference, predicted DOC concentrations are shown as dotted lines according to the same advection velocity and the same four retardation factors as for As, assuming there was no detectable DOC in the Pleistocene aquifer before the perturbation.

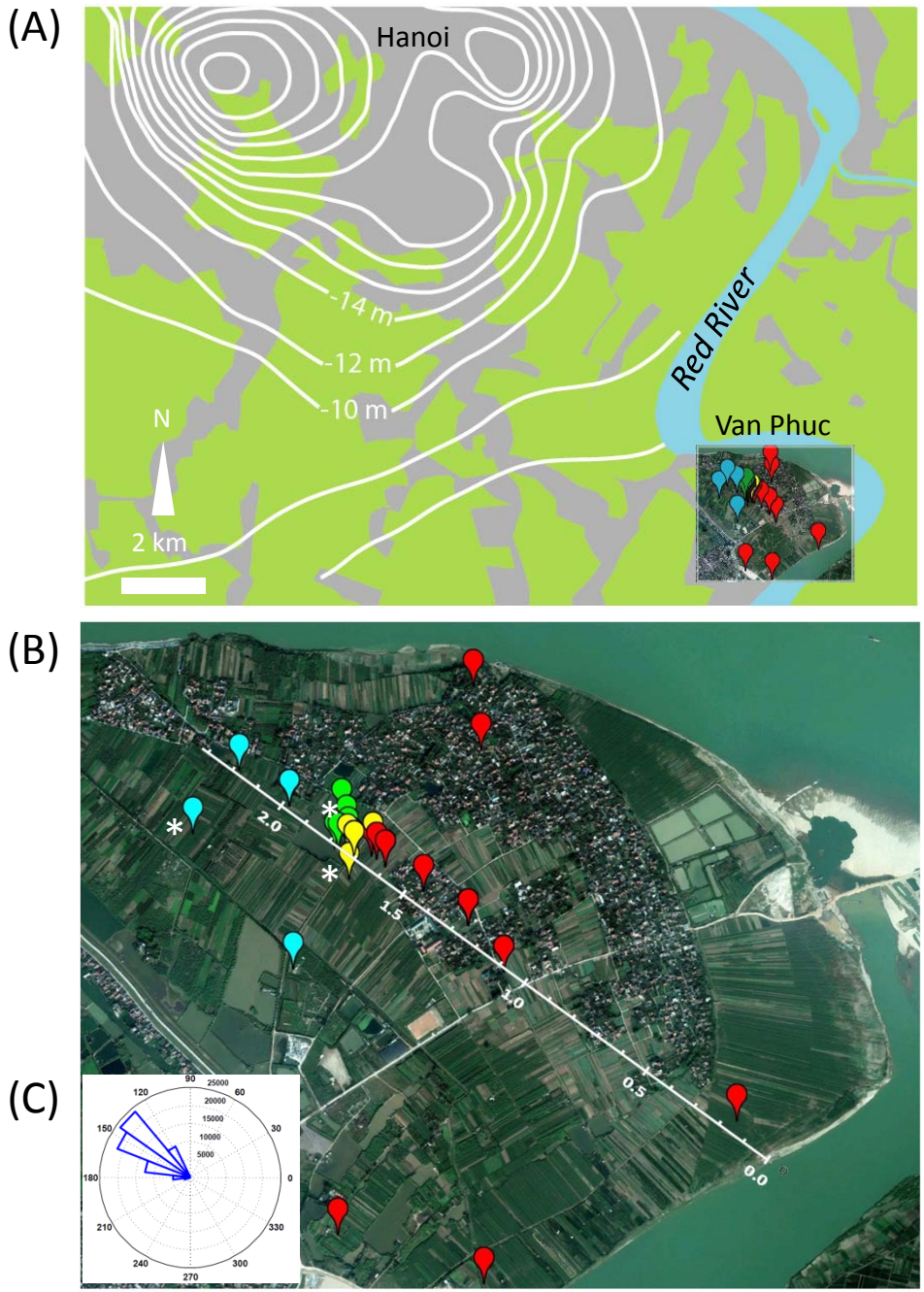
(A)
Hanoi
-14 m
-12 m
-10 m
N
2 km
Red River
Van Phuc
(B)
2.0
1.5
1.0
0.5
0.0
(C)
90
120
60
150
30
180
0
210
330
240
300
270
25000
20000
15000
10000
5000

Figure 1

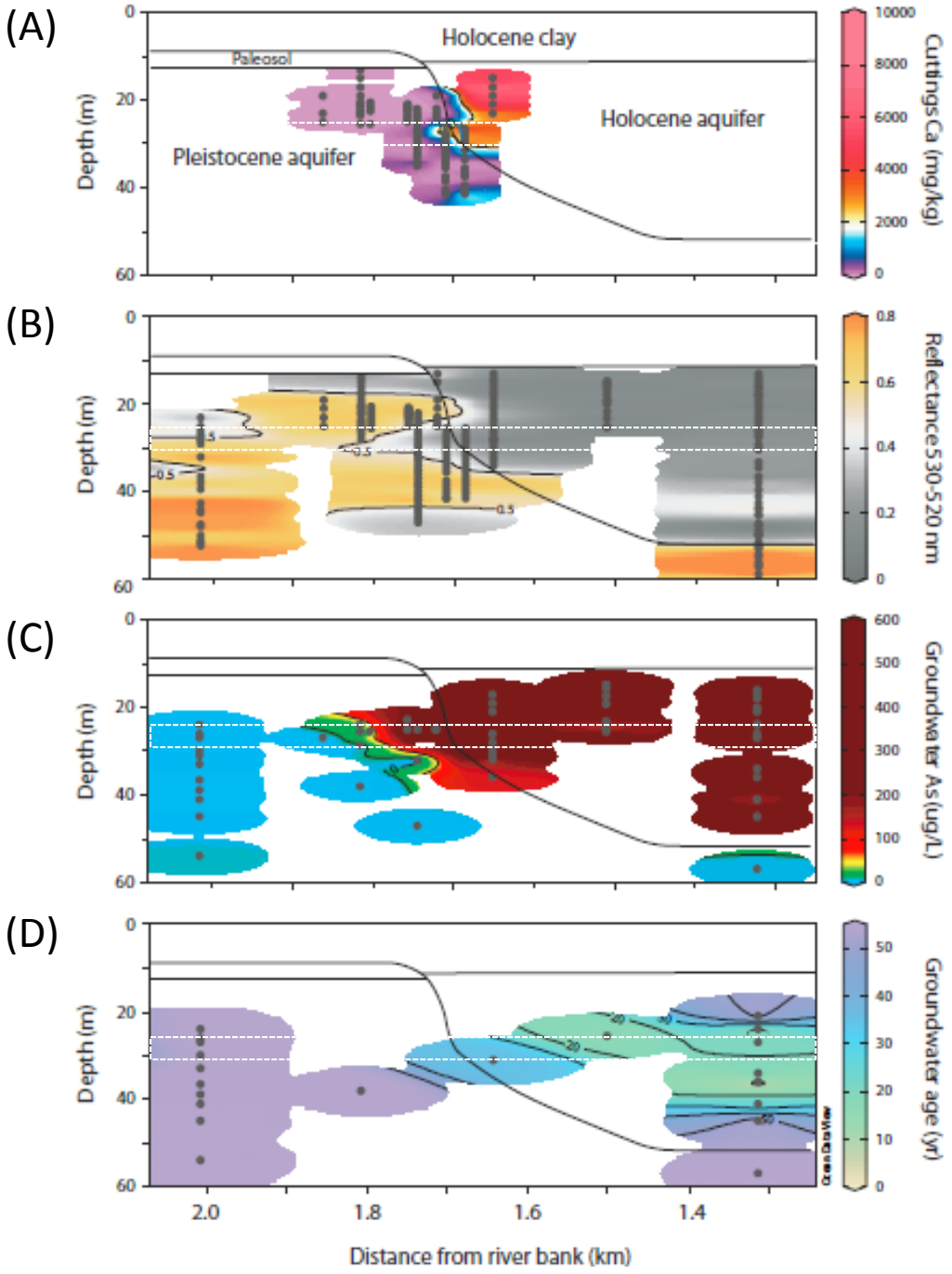
(A)
Holocene clay
Paleosol
Holocene aquifer
Pleistocene aquifer
Depth (m)
Cuttings Ca (mg/kg)
(B)
Reflectance 530-520 nm
(C)
Groundwater As (ug/L)
(D)
Groundwater age (yr)
2.0
1.8
1.6
1.4
Distance from river bank (km)

Figure 2

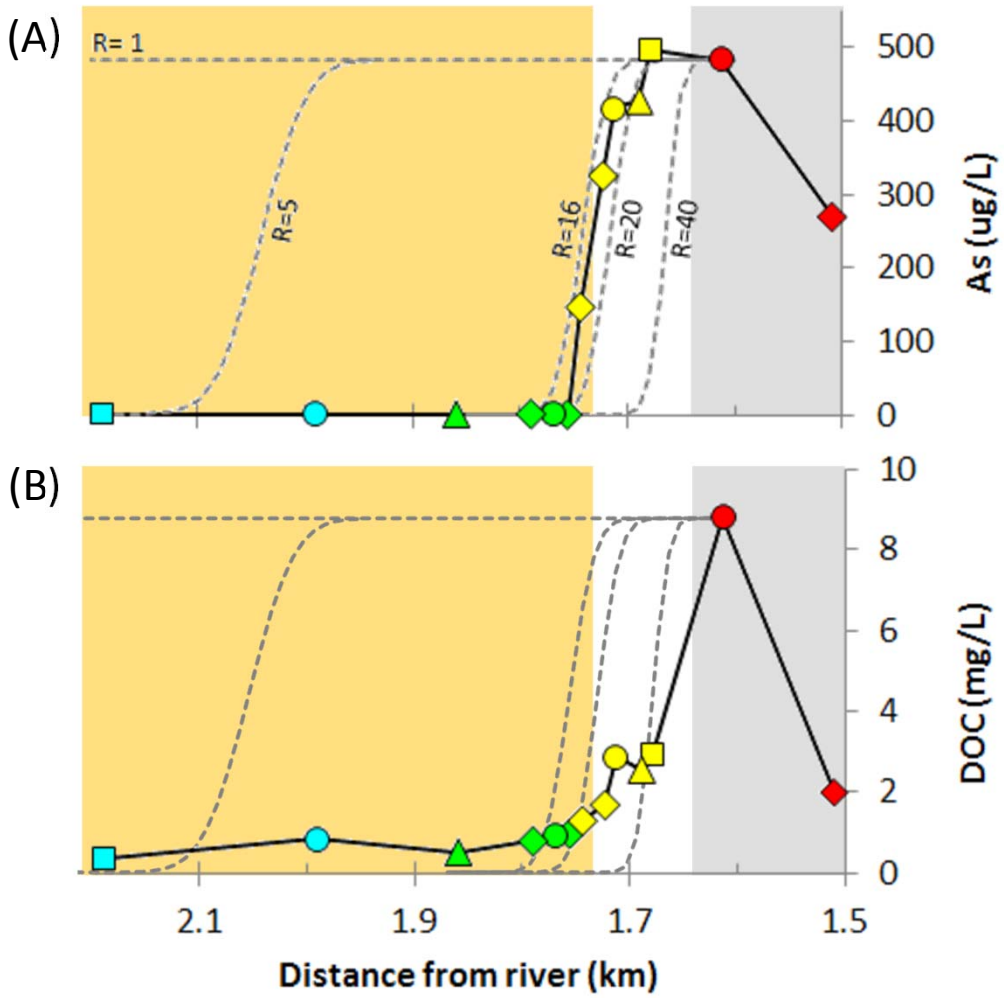
(A)
R= 1
R=5
R=16
R=20
R=40
500
400
300
200
100
0
As (ug/L)
(B)
10
8
6
4
2
0
DOC (mg/L)
2.1
1.9
1.7
1.5
Distance from river (km)

Figure 3

Methods

Drilling: A first set of 25 wells, including two nests of 9 and 10 wells each tapping the depth range of the Holocene and Pleistocene aquifers, respectively, were installed in Van Phuc in 2006 (*6*). Another 16 monitoring wells were installed between December 2009 and November 2011. Three additional holes were drilled to collect cuttings without installing a well. All holes were drilled by flushing the hole with water through a rotating drill bit.

Needle-sampling: In 2006, drilling was briefly interrupted at 7 sites to increase the vertical resolution of both sediment and groundwater data using the needle-sampler (*31*). Groundwater was pressure filtered under nitrogen directly from the sample tubes. As a measure of the pool of mobilizable As, sediment collected with the needle-sampler was subjected to a single 24-hr extraction in a 1 M PO_4 solution at pH 5 (*32*).

Water level measurements: A theodolite elevation survey of the well and river measurement points were carried out in June 2010 by a surveying team from Hanoi University of Science. Water level data in both the wells and river were recorded using Solinst Levelogger pressure transducers. A barometric pressure logger was also deployed at the field site. Water level and barometric data were recorded at 5-minute intervals and all water level data was barometrically corrected. The barometrically corrected water level data from each logger was then adjusted to the surveyed elevation of their respective measurement point so that all of the data was referenced to the same elevation datum.

Groundwater Flow: The magnitude and direction of the head gradient within the 25-30m depth of the aquifer at Van Phuc was calculated using the barometrically adjusted and survey referenced water level data collected at 5-minute intervals from September 2010 to June 2011 in three wells located near the center of the transect (Fig. 1B). A least-squares fit of a plane was calculated for each set of simultaneous water levels at these three wells, and from this set of planes the magnitude and direction of the head gradient at 5-minute intervals was directly computed.

Groundwater analysis: In 2006, a subset of the monitoring wells was sampled along a vertical transect for noble gas and tritium (^{3}H) analysis. After purging the wells, the samples were taken using a submersible pump. To avoid degassing of the groundwater due to bubble formation during sampling the water was pumped at high rates to maintain high pressure. The samples for noble gas and ^{3}H analysis were put into copper tubes and sealed gastight using pinch-off clamps. All samples were analyzed for noble gas concentrations and the isotope ratios ^{3}He/^{4}He, ^{20}Ne/^{22}Ne, and ^{36}Ar/^{40}Ar using noble gas mass spectrometry in the Noble Gas Laboratory at ETH Zurich (*30, 33*). ^{3}H concentrations were determined by the ^{3}He ingrowth method using a high-sensitivity compressor-source noble gas mass spectrometer. ^{3}H-^{3}He ages were calculated according to the equations listed in (*34*), taking into account an excess air correction. When comparing the reconstructed original ^{3}H content of each sample as a function of ^{3}H-^{3}He age with the ^{3}H input function for South and Southeast Asia (Fig. S5), most samples follow the trend expected from simple plug flow (*34-35*).

Several days before analysis by high-resolution inductively-coupled plasma mass spectrometry (HR ICP-MS) at LDEO, groundwater was acidified to 1% Optima HCl in the laboratory (*36*).

This has been shown to entirely re-dissolve any precipitates that could have formed (*37*). In most cases, the difference between duplicates was within the analytical uncertainty of ~5%. With the exception of needle-sample data and the nest of 10 wells in the Holocene portion of the aquifer, which had to yield to construction, groundwater As, Fe, and Mn concentrations reported here represent the average for samples collected without filtration in April and May 2012. Groundwater data from 2006 were previously reported in (*6*) and (*31*).

Dissolved organic carbon (DOC) samples were collected in 25 mL glass vials combusted overnight at 450 ^{o}C and acidified to 1% HCl at the time of collection. Dissolved inorganic carbon (DIC) samples were also collected in 25 mL glass vials with a Teflon septum but were not acidified. Both DOC ("NPOC") and DIC (by difference of "TC-NPOC") were analyzed on a Shimadzu TOC-V carbon analyzer calibrated with K phthalate standards.

Ammonium samples were collected in polypropylene bottles after passing through 0.45 um cellulose acetate membrane filters and preserved by acidifying to pH<2 with HNO_3. NH_4^+ concentrations were analyzed on a spectrophotmeter (UV-3101, Shimadzu) at a wavelength of 690 nm after forming complex with nitroferricyanide (*38*).

Methane (CH_4) samples were filled up to about half of the pre-vacuumed glass vials and immediately frozen in dry ice. The analyses were performed no longer than 10 days after sampling. Headspace CH_4 in the vials was measured on a Shimadzu 2014 gas chromatography with a Porapak T packed column (*14*).

Sediment analysis: As a measure of the redox state of Fe in acid-leachable oxyhydroxides, the diffuse spectral reflectance spectrum of cuttings from at all sites was measured on samples wrapped in Saran wrap and kept out of the sun within 12 hours of collection using a Minolta 1600D instrument (*13*). Starting in 2009, the coarse fraction of the drill cuttings were analyzed by X-ray fluorescence for a suite of elements including Ca using an InnovX Delta instrument. The drill cuttings were resuspended in water several times to eliminate the overprint of Ca-enriched clays contained in the recycled water used for drilling. The washed samples were run as is, without drying or grinding to powder. Analyses of NIST reference material SRM2711 (28,800 ± 800 mg/kg Ca) analyzed by X-ray fluorescence at the beginning and end of each run averaged 30,200 ± 400 mg/kg (n=16).

Methods References

31. van Geen, A. *et al.* Comparison of arsenic concentrations in simultaneously-collected groundwater and aquifer particles from Bangladesh, India, Vietnam, and Nepal. *Applied Geochemistry* **23**, 3244-3251 (2008).
32. Zheng, Y. *et al.*, Geochemical and hydrogeological contrasts between shallow and deeper aquifers in two villages of Araihazar, Bangladesh: Implications for deeper aquifers as drinking water sources. *Geochim. Cosmochim. Acta* **69**, 5203-5218 (2005).
33. Frei, F. Groundwater dynamics and arsenic mobilization near Hanoi (Vietnam) assessed using noble gases and tritium. Diploma thesis, ETH Zurich (2007).
34. Klump, S. *et al.* Groundwater dynamics and arsenic mobilization in Bangladesh assessed using noble gases and tritium. *Environ. Sci. Technol.* **40**, 243-250 (2006).

35. Stute, M. *et al.* Hydrological control of As concentrations in Bangladesh groundwater.*Water Resources Research,* **43** doi:10.1029/2005WR004499 (2007).
36. Cheng, Z., Zheng, Y., Mortlock, R., & van Geen, A. Rapid multi-element analysis of groundwater by high-resolution inductively coupled plasma mass spectrometry. *Analytical* and Bioanalytical Chemistry **379**, 513-518 (2004).
37. van Geen *et al.* Monitoring 51 deep community wells in Araihazar, Bangladesh, for up to 5 years: Implications for arsenic mitigation, *Journal of Environmental Science and Health Part A* **42**, 1729-1740 (2007).
38. Koroleff, F. *Methods of Seawater Analysis* (K. Grasshoft, ed.). Verlag Chemie (1976).

Supplementary Information

Retardation of arsenic transport through a Pleistocene aquifer

Alexander van Geen[1], Benjamín C. Bostick[1], Pham Thi Kim Trang[2], Vi Mai Lan[2], Nguyen-Ngoc Mai[2], Phu Dao Manh[2], Pham Hung Viet[2], Kathleen Radloff[1], Zahid Aziz[1], Jacob L. Mey[1], Mason O. Stahl[3], Charles F. Harvey[3], Peter Oates[4], Beth Weinman[5], Caroline Stengel[6], Felix Frei[6], Rolf Kipfer[6], Michael Berg[6]

[1]Lamont-Doherty Earth Observatory of Columbia University, Palisades, NY 10964, USA
[2]CETASD, Hanoi University of Science, Vietnam National University, Hanoi, Vietnam
[3]Massachusetts Institute of Technology, Cambridge, MA 02139, USA
[4]Anchor QEA, LLC, Montvale, NJ 07645, USA
[5]Earth & Environmental Sciences, Vanderbilt University, Nashville, TN 37235, USA
[6]Eawag, Swiss Federal Institute of Aquatic Science and Technology, Dübendorf, Switzerland

SI Guide

The Supplementary Information includes 8 figures referred to in the main text and a supplementary discussion of groundwater-age modeling, a derivation of the age-distance relationship, a description of additional changes in chemistry across the geological front of the village, the equation used to calculate retardation, and a table with all the groundwater noble gas, ^{3}H, and ^{3}H-^{3}He age data.

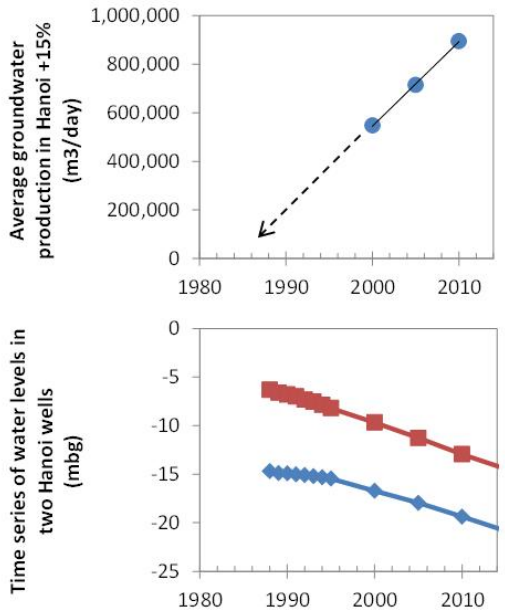

Figure S1 (A) Government estimates of total municipal pumping in 2000 and 2005, with a projection for 2010 provided in 2006 by the Hanoi Water Works. (B) Water levels in the Phapvan (red) and Maidich (blue) well fields of Hanoi used to model subsidence (*9*).

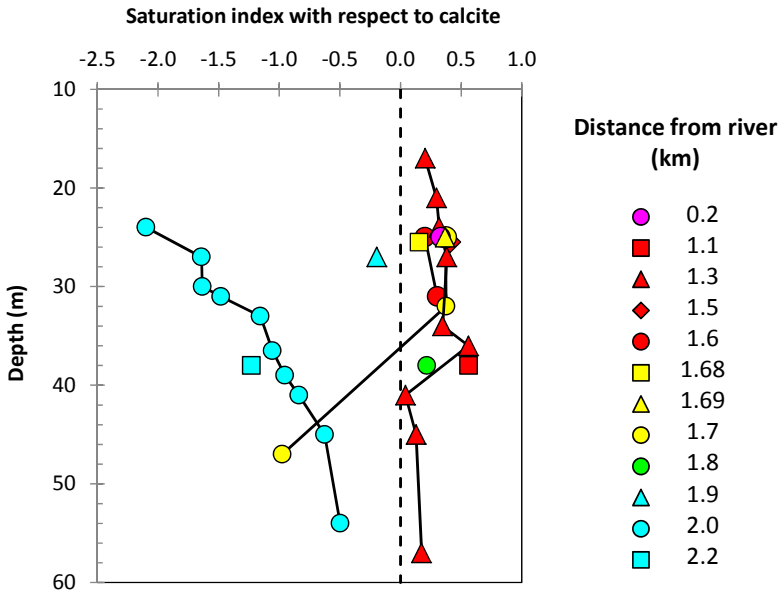

Figure S2 Saturation index with respect to calcite calculated using Visual MINTEQ 3.0 (http://www2.lwr.kth.se/English/OurSoftware/vminteq/) on the basis of concentrations of Ca, alkalinity and pH measured in groundwater from the Pleistocene and Holocene aquifers of Van Phuc. Symbols shapes and colors as in Fig. 3. Similar calculations for dolomite are presented in (*6*).

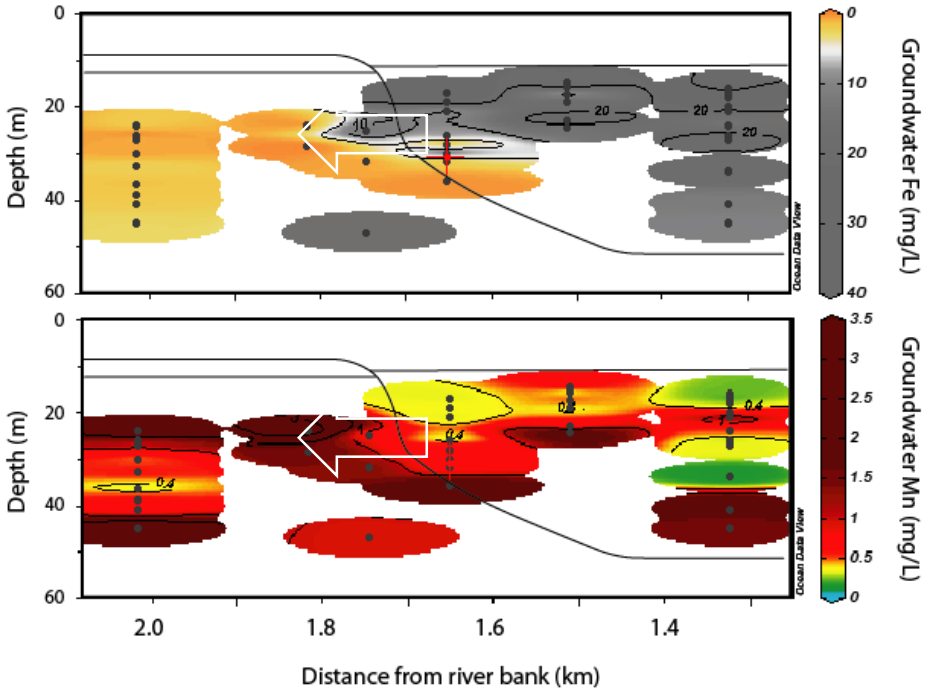

Figure S3 Contoured sections of groundwater (A) Fe and (B) Mn concentrations between distances of 1.3 and 2.0 km from the Red River bank. Also shown are the boundary separating the two main aquifers and the paleosol overlying the Pleistocene aquifer. The portion of the Pleistocene aquifer that became reduced and where As concentrations presumably increased over time is located within the large arrow pointing in the direction of flow.

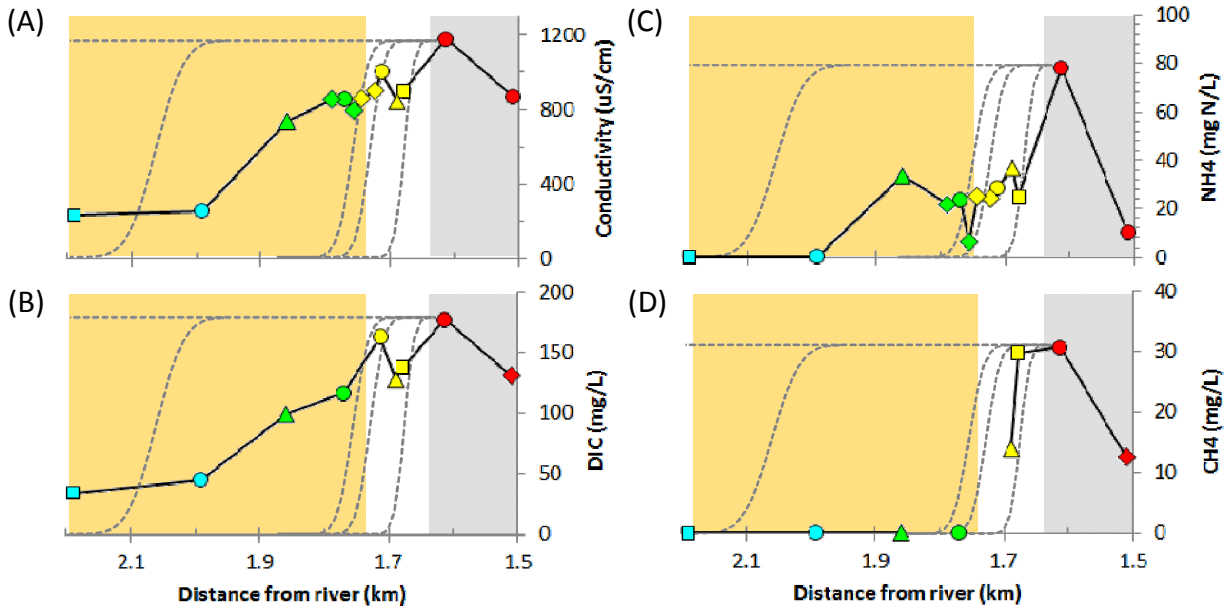

Figure S4 Distribution of (A) conductivity, (B) dissolved inorganic carbon (DIC), (C) ammonium (NH_4^+), and (D) methane (CH_4) within the 25-30 m depth interval along the Van Phuc transect. Symbols are colored according to the classification in Fig. 1. Grey and yellow shading indicates the extent of the grey Holocene aquifer and the portion of the Pleistocene aquifer that is still orange, respectively. The intermediate area without shading indicates the portion of the Pleistocene aquifer that turned grey. For visual reference, predicted conductivity and concentrations in groundwater are shown as dotted lines according to an average advection velocity 43 m/yr over 50 years using a 5-40 range of retardation as well as the 16-20 range calculated for As from this study.

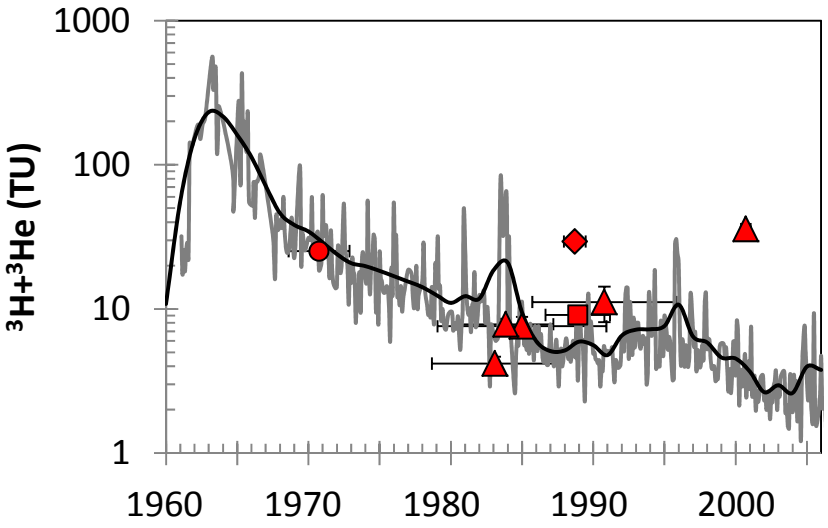

Figure S5 Comparison of sum of ^3H and ^3He levels and this "stable ^3H" with predicted levels based on the history of bomb input and dispersion. For 3 out of the 8 samples along the transect that were dated, stable ^3H levels significantly deviate from the model, presumably because of mixing and/or deviation from simple plug flow. The single point with a deficit in stable ^3H could be due to mixing with old water recharged before the 1950s (*35*) whereas the two points elevated in stable ^3H may reflect mixing with a component of groundwater recharged in the 1960-1970 when the levels of ^3H in precipitation were particularly high. For one additional sample, problems were already recorded during the analysis and the measurement was not taken into account (*33*).

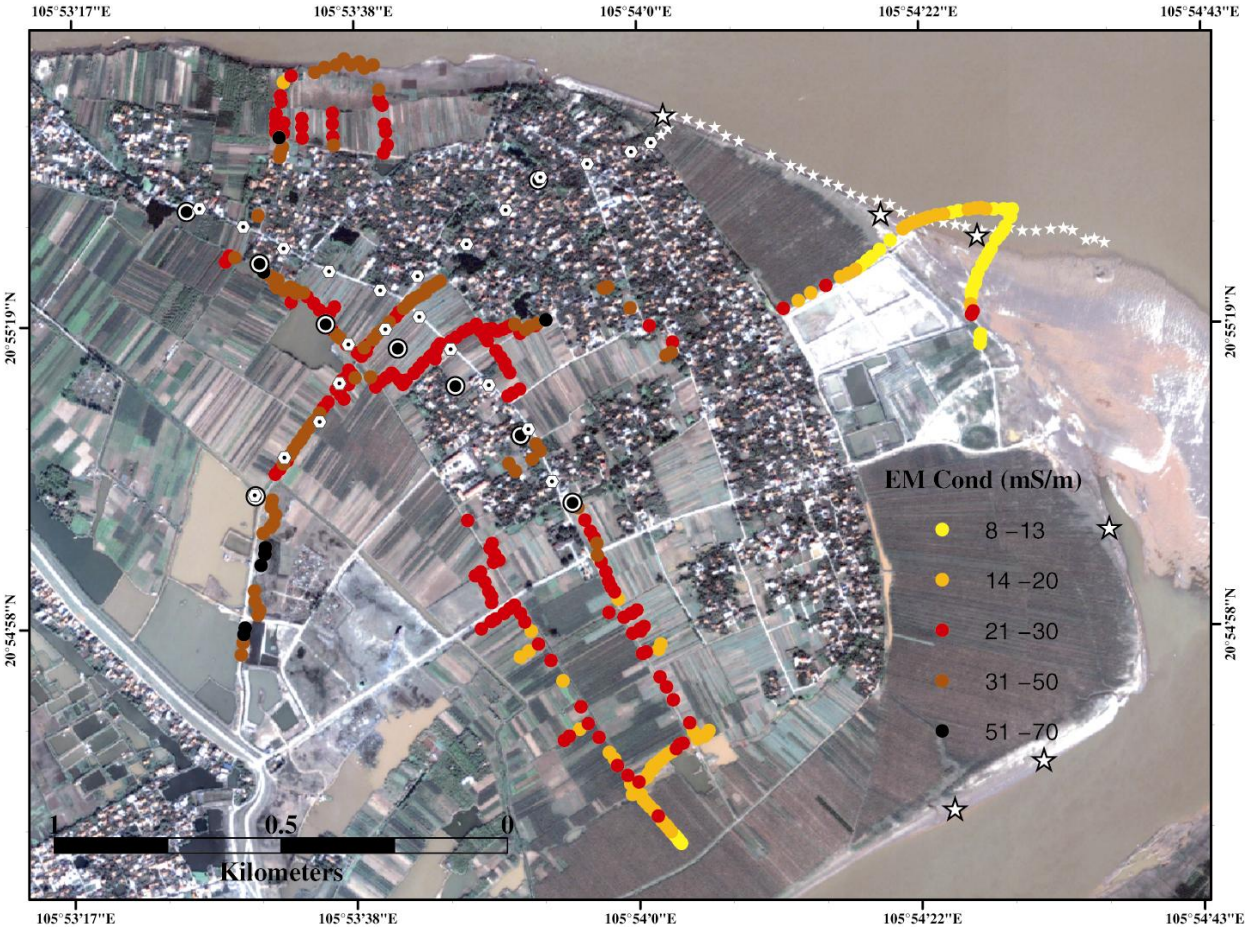

Figure S6 Variations in EM conductivity across the Red River meander of Van Phuc. Areas of low EM conductivity indicate proximity to the surface of sand; areas of high EM conductivity correspond to a thick surficial clay layer (*39*).

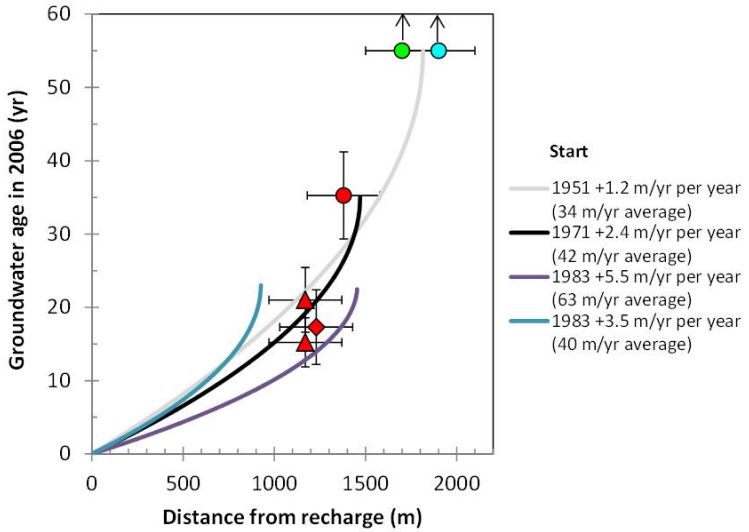

Figure S7 Prediction of the distribution of groundwater age in 2006 as a function of distance from the southern river bank of Van Phuc for different groundwater flow scenarios (see Supplementary Discussion). Horizontal error bars span the 400 m width of the likely recharge area. Vertical error bars indicate the measurement error in groundwater ages. Symbols are colored according to the classification in Fig. 1. Samples without detectable ^{3}H are shown assuming the minimum age of 55 years. Solid lines indicate predicted age-distance relationships for various combinations of start dates and annual increments for enhanced groundwater flow attributable to Hanoi pumping.

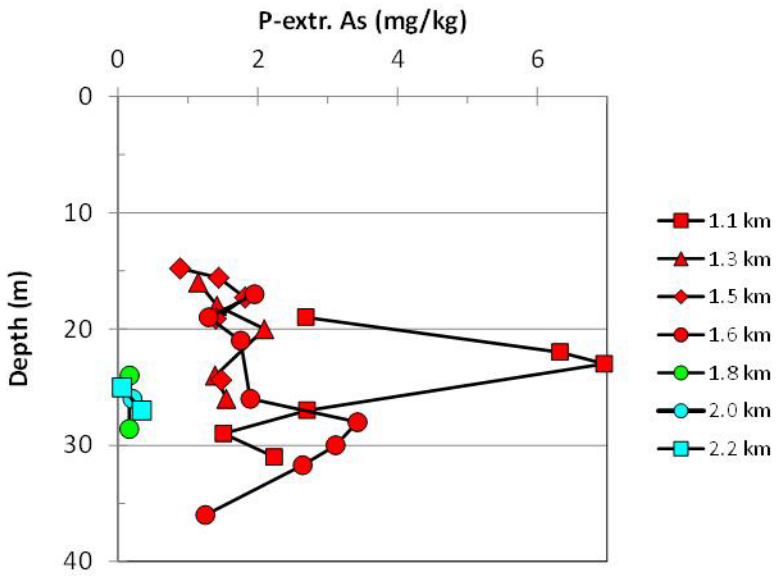

Figure S8 Phosphate-extractable As levels in Holocene and Pleistocene sediment collected with the needle-sampler in 2006, from (*31*) and additional data for orange Pleistocene aquifer (green and blue symbols). Despite the contrast in P-extractable As between the two formations, the extent to which the contamination was caused by As transport from the adjacent Holocene aquifer or reductive dissolution of Fe(III) oxyhydroxides and *in situ* As release to groundwater cannot be determined. Release of ~0.2 mg/kg As from the Pleistocene sands following the reduction of Fe oxyhydroxides could result in an increase in groundwater As concentrations by as much as 500 μg/L (*2*).

Supplementary Discussion

Groundwater Age Modeling: The mean age and ^{3}H-^{3}He age for the different pumping scenarios outlined in the paper were solved numerically to test how dispersion could influence the results. The average difference over the modeled domain between the analytical solution for groundwater ages and the numerical solution for mean groundwater ages was less than one-percent for all of the modeled scenarios. The average difference over the modeled domain between the numerical solution for ^{3}H-^{3}He ages and the analytical solution for the groundwater ages was less than 10-percent for all the modeled scenarios. Comparison of these numerical solutions that include dispersion with the analytic solution for purely advective transport indicate that dispersion had a small effect on the calculated ages.

The one-dimensional advective-dispersive equation with a reaction term for the aging process was evaluated using finite-volumes with an explicit time-stepping method. In each scenario the initial velocity was set equal to zero and the velocity in all subsequent time-steps was assigned according to the groundwater acceleration rate for the scenario being modeled. A dispersivity value of 5m, representative of a sandy aquifer, was used in all of the modeled scenarios. For the mean age calculations the inflowing water was assigned an age of zero. In case of the ^{3}H-^{3}He age calculations, atmospheric tritium data reported monthly by the IAEA from 1961 to 2009 for Hong Kong were used to assign tritium values to the inflowing water (IAEA/WMO (2006). Global Network of Isotopes in Precipitation. The GNIP Database. Accessible at: http://www.iaea.org/water). Mean age calculations for each pumping scenario were run for two different sets of initial conditions. In the first case the initial ages were set equal to zero throughout the modeled domain. In the second case the initial ages throughout the domain were set equal to 200 years, a reasonable age estimate at 30 m-depth in the aquifer under conditions of only vertical groundwater recharge that likely dominated prior to the influence of pumping.

EQ1 was used solved numerically to model the mean groundwater ages and EQ2 and EQ3 were solved numerically to model the He-Tritium ages of the groundwater:

$$(EQ1): \frac{\partial A}{\partial t} = -V\frac{\partial A}{\partial x} + (V * \alpha)\frac{\partial^2 A}{\partial x^2} + R$$

$$(EQ2): \frac{\partial Tr}{\partial t} = -V\frac{\partial Tr}{\partial x} + (V * \alpha)\frac{\partial^2 Tr}{\partial x^2} - K * Tr$$

$$(EQ3): \frac{\partial He}{\partial t} = -V\frac{\partial He}{\partial x} + (V * \alpha)\frac{\partial^2 He}{\partial x^2} + K * Tr$$

Where A is age [T]; V is velocity [L/T]; α is dispersivity [L]; R is the aging constant [dimensionless]; Tr is the tritium activity [TU]; K is the tritium decay constant [1/T]; He is the tritiogenic ^{3}He concentration, i.e. the ^{3}He that is produced by ^{3}H decay [TU].

Reconstruction of past flow induced by pumping:

The main source of recharge must be known in order to relate ^{3}H-^{3}He ages to groundwater flow velocities. Recharge of the Van Phuc aquifer could enter directly from the sandy river bottom or enter the aquifer above the river bank during flooding of low-lying areas, which occurred as recently as 2002 even though the level of the Red River is largely controlled upstream by a series of dams. A geophysical survey of the area combined with drilling logs shows that the sandy

aquifer extends almost to the surface in the eastern uninhabited portions of the meander and, unlike most of the remaining area, is not capped by a thick clay layer (Fig. S6). On the basis of these observations, the likely recharge area for the groundwater sampled along the transect extends from the center of the Red River to the inland area where the surficial clay layer thickens markedly, i.e. from 100 m southeast to 300 m northwest of the river bank (Fig. 1B).

The increase in ^{3}H-^{3}He groundwater age with travel distance from the recharge area is used to estimate how groundwater velocity has shifted in recent decades. The distribution of groundwater ages along the transect indicates that the rate of recharge of the aquifer at the river has not been constant (Fig. S7). Time series of groundwater level indicate a roughly linear increase in the depth of the cone of depression below Hanoi since at least 1988 and imply a constant acceleration of groundwater flow over time (Fig. S1). Steady flow divergence could also explain the apparent decrease in velocity along the transect, but this interpretation is inconsistent with pressure transducer records at the geological boundary. The simplest explanation for the observed distribution of ages as a function of distance from the recharge area is therefore accelerating flow drawn by increased Hanoi pumping.

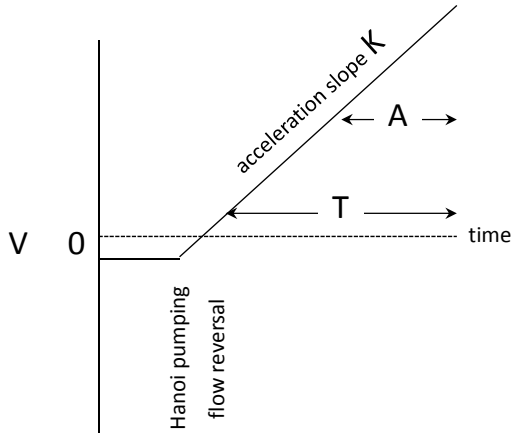

On the basis of this assumption and neglecting dispersion, the distance of the front from recharge at the upstream end of the transect is $X_F = KT^2/2$, where K is the slope of the acceleration and T is the time since the gradient reversal, calculated by integrating the expression $Vdt = Kt\,dt$ from time zero to time T. In order to calculate the groundwater age A of the water behind the front (i.e. $X<X_F$), the same expression is integrated from time T-A to time T and solved for $A = T - (T^2 - 2X/K)^{1/2}$. A numerical model including Fickian dispersion shows that the age-distance relation is not particularly sensitive to dispersion. Two model scenarios illustrated in Fig. S7 reflect government pumping rate estimates which back-extrapolate linearly to zero groundwater extraction in 1983 (Fig. S1). Annual increases in groundwater velocities by 3.5 and 5.5 m/yr starting in 1983, respectively, encompass the envelope of distances and ages defined by the 3 samples within the faster moving core (24-28 m depth). Although economic liberalization in Vietnam and, therefore possibly an increase in municipal pumping, started in the early 1980s, the two scenarios do not seem plausible because groundwater pumping reportedly started in Hanoi as early as 1909 (*9*). In addition, a 1983 start date for the perturbation cannot generate groundwater that has been isolated from the atmosphere for more than 23 years (the 2006 sampling date minus the presumed 1983 onset of intense groundwater pumping) and therefore do

not extend to the sample of 35-yr-old water at 32 m depth and a distance of 1380 m from the recharge area (Fig. S7).

A scenario that fits the range of all groundwater ages measured by the ^{3}H-^{3}He method requires a reversal of the head gradient taking place in Van Phuc no later than 1971 and, therefore, a slower annual increase in advection of 2.4 m/yr (Fig. S7). The 1971 reversal date corresponds roughly to the end of what is referred to in Vietnam as the American War. In order to extend the model to the minimum age of 55 yr established for groundwater in the Pleistocene aquifer, the reversal of flow directions has to be anticipated by another 20 years to 1951 and the annual increase reduced to 1.2 m/yr. Advection velocities of 75 and 95 m/yr in 2010 predicted for flow reversals starting in 1951 or 1971, respectively, combined with the average head gradient measured in Van Phuc in 2010-11 of 5.2×10^{-4} (Fig. 1C), yield hydraulic conductivities of 100-125 m/day (assuming a porosity = 0.25) that are within the range expected for sandy aquifers. The two transient flow models yield average advection rates of 38 and 48 m/yr, respectively, over the time spans of 40 and 60 years separating the onset of the flow perturbation and groundwater sampling for chemical analysis in 2011.

Changes in groundwater chemistry across the Holocene-Pleistocene boundary:

The single most abundant constituent of Van Phuc groundwater is dissolved inorganic carbon (DIC), primarily in the form of bicarbonate ion (Fig. S4). Given the circumneutral pH of groundwater, the distribution of DIC and conductivity are therefore closely coupled. Much lower concentrations of DIC, methane (CH_4), and ammonium (NH_4^+) in the Pleistocene portion of the Van Phuc transect compared to the Holocene are consistent with the association between sediment age and organic matter reactivity recently documented elsewhere in the Red River basin (*14*). DIC is present at an order of magnitude higher concentration than DOC and therefore unlikely to be significantly enhanced by DOC remineralization along the transect. Some contribution to the sharp drop in DOC as groundwater crosses the geological boundary due to adsorption onto the sediment cannot be ruled out, although field observations indicate retardation of DOC is not likely to be as pronounced as for As (*40*). Other groundwater constituents elevated in the Holocene portion of the aquifer such as DIC and NH_4^+ migrated at least twice as far as As into the Pleistocene aquifer (Fig. S4).

Although surface-complexation models have been developed to predict the retardation of As due to adsorption in both Holocene and Pleistocene sands (e.g. *22*), the available data do not justify assumptions beyond that of a linear adsorption isotherm described by a distribution coefficient K_d that is the ratio of the As concentration in the particulate phase per mass of sediment divided by the As concentration in the dissolved phase (*18*). For a simple one-dimensional advection-diffusion model that assumes no As is initially present along the flow path and that recharge water enters the aquifer at one end of the flow path containing an As concentration C_i, the solution of the governing equation is:

$$C(x,t) = C_i\left[1 - \frac{1}{2}\mathrm{erfc}\frac{(Rx - vt)}{2(DRt)^{\frac{1}{2}}} + \frac{1}{2}\exp(vx/D)erfc\frac{(Rx + vt)}{2(DRt)^{\frac{1}{2}}}\right]$$

where C is the concentration of As in the dissolved phase, x the distance along the flow path, v the advection velocity, D is a hydraulic dispersion coefficient, and R the retardation factor (*41*). Assuming As initial concentrations of 486 μg/L in the Holocene aquifer at a distance of 1.6 km from the river bank and 1 μg/L of Pleistocene aquifer, two retardation factors R but the same dispersion coefficient D were calculated for the two advection scenarios by iteratively minimizing the sum of the squared residuals between the observations and the model predictions. For an optimized hydraulic dispersion of 1.8 10^{-6} m^2/s, retardation factors of 16 and 20 are calculated for advection at 48 m/yr for 40 years and at 38 m/yr for 60 years, respectively. The trends in predicted As concentrations based on these two scenarios are essentially indistinguishable. The same retardation factors were applied to an average advection scenario of 43 m/yr for 50 years to illustrate that they span the likely range of uncertainty in As retardation (Fig. 3). The distribution coefficient K_d is related to the retardation factor R by the equation $K_d = \theta/\rho\ (R-1)$, where θ is a typical aquifer porosity of 0.25 and ρ is the corresponding aquifer bulk density assuming a dry sediment density of 2.65 kg/cm^3. With these assumptions, retardation factors of 16-20 are equivalent to distribution coefficients of 1.7-2.1 L/kg.

The pattern of Ca concentrations in sand cuttings provides an independent check on groundwater flow across the Holocene-Pleistocene boundary in Van Phuc. Detrital carbonate is rarely observed in fluvial sediment, even in karstic terrain such as the Red River watershed. Unlike the Pleistocene aquifer, groundwater within the Holocene aquifer of Van Phuc is highly supersaturated with respect to calcite due to a combination of elevated Ca (2 mmol/L) and DIC concentrations (10 mmol/L) at pH 7 driven by the metabolism of organic carbon paired with reductive dissolution of Fe oxyhydroxides (Fig. S2). Elevated Ca concentrations in Holocene sand cuttings of Van Phuc therefore most likely indicates authigenic precipitation of calcite or dolomite. The deficit in conductivity and DIC between 1.7 and 1.9 km from the river bank relative to the model prediction may indicate that, in addition to adsorption of DIC, some precipitation of calcite occurs as groundwater from the Holocene aquifer enters the Pleistocene aquifer (Fig. S4). This process provides an independent check on the onset of strong northwesterly groundwater flow in Van Phuc. On the basis of the Ca concentration in the northernmost well tapping the Holocene aquifer, precipitation from almost 1000 pore volumes of advected groundwater would be required to build up a concentration of 2000 mg/kg Ca in the sediment. Given the 2 km advection of the groundwater front, elevated Ca concentrations in cuttings would not be expected beyond a few meters downstream of the Holocene-Pleistocene transition even if calcite precipitation were very rapid. The lack of detectable Ca in cuttings from the first set of wells within the Pleistocene aquifer that are contaminated with As is therefore consistent with a recent acceleration of northwesterly flow.

Supplementary References

39. Aziz, Z. *et al.* Impact of local recharge on arsenic concentrations in shallow aquifers inferred from the electromagnetic conductivity of soils in Araihazar, Bangladesh, *Water Resources Research* **44**, doi:10.1029/2007WR006000 (2008).
40. McCarthy, J. F. *et al.* Field tracer tests on the mobility of natural organic matter in a sandy aquifer. *Water Resources Research* **32**, 1223-1238 (1996).
41. van Genuchten, M. Th. & Alves, W. J. Analytical solutions of the one-dimensional convective-dispersive solute transport equation; USDAARS Technical Bulletin 1661; U.S. Salinity Laboratory: Riverside, CA (1982).

Table S1. Noble gas and ^{3}H data

Well	Latitude	Longitude	Depth (m)	He	+/-	Δ Ne	Δ Ar	$^{3}He/^{4}He$	+/-	$^{20}Ne/^{22}Ne$	+/-	$^{40}Ar/^{36}Ar$	+/-	$^{3}He_{tri}$	+/-	^{3}H	+/-	^{3}H-^{3}He age	+/-
				(10^{-8} cm^{3}_{STP}/g)		(%)	(%)	(10^{-6})				(10^{2})		(TU)		(TU)		(yr)	
MLA1	20.92326	105.89198	24	1.70	0.02	-71	-67	1.29	0.02	9.81	0.07	2.98	0.02	1.87	0.22	0.0	0.6	>55	
MLA2	20.92326	105.89198	27	1.93	0.02	-68	-68	1.33	0.02	9.85	0.04	2.93	0.02	1.82	0.18	-	-	(>55)	
MLA3	20.92326	105.89198	30	1.93	0.02	-68	-68	1.33	0.02	9.83	0.03	2.95	<0.01	1.81	0.19	0.0	1.4	>55	
MLA4	20.92326	105.89198	33	2.24	0.02	-49	-27	1.39	0.02	9.88	0.04	2.92	0.01	1.16	0.21	0.0	0.5	>55	
MLA5	20.92326	105.89198	36	2.66	0.03	-35	-16	-	-	9.81	0.02	2.96	0.01	-	-	0.4	1.0	>55	
MLA6	20.92326	105.89198	39	2.44	0.02	-38	-20	1.35	0.01	9.77	0.03	2.96	0.01	0	0.22	-	-	(>55)	
MLA7	20.92326	105.89198	41	2.55	0.03	-35	-17	1.35	0.02	9.79	0.01	2.96	0.01	0	0.26	0.2	0.4	>55	
MLA8	20.92326	105.89198	45	2.12	0.02	-58	-57	1.32	0.02	9.79	0.03	2.95	0.01	0.28	-	0.0	0.6	>55	
MLAC	20.92326	105.89198	54	2.11	0.02	-60	-48	1.25	0.02	9.82	0.03	2.97	0.01	1.18	-	0.0	2.2	>55	
MLB2	20.91982	105.89751	21	3.66	0.04	-14	-4	1.92	0.02	9.75	0.04	2.94	0.01	7.73	2.04	0.0	1.1	>55	
MLB3	20.91982	105.89751	24	3.79	0.04	-13	-3	1.80	0.01	9.79	0.02	2.96	<0.01	6.41	2.94	4.8	0.9	15.2	5.1
MLB4	20.91982	105.89751	27	4.95	0.05	11	10	1.64	0.02	9.80	0.01	2.96	<0.01	5.25	0.58	2.3	1.1	21.0	5.9
MLB5	20.91982	105.89751	34	5.16	0.05	16	13	1.64	0.01	9.78	0.02	2.96	<0.01	5.56	0.42	2.3	0.6	22.2	3.4
MLB6	20.91982	105.89751	36	5.02	0.05	17	15	1.88	0.01	9.78	0.01	2.96	<0.01	9.17	0.5	26.7	1.2	5.3	0.3
MLB7	20.91982	105.89751	41	3.32	0.03	-21	-11	1.63	0.01	9.77	0.02	2.96	0.01	3.02	0.29	1.2	0.4	22.9	4.4
MLB8	20.91982	105.89751	45	3.53	0.04	-17	-7	1.64	0.01	9.79	0.02	2.95	<0.01	3.63	0.34	0.0	1.2	>55	
MLBC	20.91982	105.89751	57	3.10	0.03	-30	-6	1.31	0.01	9.82	0.01	2.95	<0.01	0	-	0.2	1.0	>55	
NS3	20.92081	105.89613	26	4.59	0.05	4	7	2.41	0.02	9.77	0.01	2.96	0.01	18.25	0.74	11.2	0.6	17.3	0.8
NS9	20.92489	105.89791	26	6.23	0.06	40	17	1.62	0.01	9.78	0.01	2.97	<0.01	5.59	0.73	3.5	0.6	17.1	2.3
NS6	20.92429	105.89043	28	3.55	0.04	-19	-11	1.43	0.01	9.80	0.01	2.95	0.01	1.37	(> 1.37)	4.6	0.9	4.6	(> 4.1)
NS5	20.92152	105.89495	31	4.92	0.05	14	14	2.53	0.02	9.77	0.02	2.95	0.01	21.7	0.54	3.5	0.5	35.3	2.1
NS1	20.92326	105.89198	31	5.34	0.05	14	-1	1.31	0.01	9.83	0.02	2.95	0.01	4.18	-	0.0	0.6	>55	
NS4	20.92205	105.89338	38	4.80	0.05	9	9	1.36	0.01	9.76	0.01	2.96	<0.01	0	0.5	0.1	0.6	>55	